Entropy gives rise to topologically associating domains

Paula A. Vasquez[1], Caitlin Hult[2], David Adalsteinsson[2], Josh Lawrimore[3], Mark G. Forest[2] and Kerry Bloom[3,*]

[1]Department of Mathematics, University of South Carolina, Columbia, SC 29808, USA, [2]Department of Mathematics, University of North Carolina, Chapel Hill, NC 27599, USA and [3]Department of Biology, University of North Carolina, Chapel Hill, NC 27599, USA

ABSTRACT

We investigate chromosome organization within the nucleus using polymer models whose formulation is closely guided by experiments in live yeast cells. We employ bead-spring chromosome models together with loop formation within the chains and the presence of nuclear bodies to quantify the extent to which these mechanisms shape the topological landscape in the interphase nucleus. By investigating the genome as a dynamical system, we show that domains of high chromosomal interactions can arise solely from the polymeric nature of the chromosome arms due to entropic interactions and nuclear confinement. In this view, the role of bio-chemical related processes is to modulate and extend the duration of the interacting domains.

INTRODUCTION

The genome comprises the entire genetic information that makes up an organism. This information is encoded in DNA and stored, spatially and dynamically, in the nucleus of every cell in that organism. Packaging while preserving functionality of DNA in the nucleus is one of the most remarkable tasks performed by cells. To accomplish this task, the cell employs hierarchical levels of compaction and organization. Understanding the spatial dynamics of the genome is a crucial step in characterizing how DNA adopts and transitions between different functional states over the course of the cell cycle, facilitating vital functions such as gene expression, DNA replication, recombination and repair. Today, advances in instrumentation, experimental techniques, theory and computation are poised for integration toward a predictive description of the structural organization and dynamics of the living genome, and for understanding the entropy-dominated statistical mechanics underpinning different cellular functions. Toward this goal, we hypothesize that in the nucleus, thermodynamics, in par-

ticular entropy, dominates the spatial organization of chromosome arms while active kinetic processes modulate this organization. This view represents a shift from that of enzymatic, biochemical cellular processes playing the leading role in these cell functions. In short, enzymes do not create a new topological and energetic landscape in the nucleus; rather they bias the entropy-dominated stochastic dynamics into cycle-specific states. Here we show that entropy and confinement dictate the leading order structure and dynamics of the genome, whereas the role of enzymes is to guide, stabilize and sustain cycle-specific genome states.

The organization of the genome in the nucleus can be divided into three length scales (1). At the lower scale, between 1 base pair (bp) and several thousand base pairs (kb), the genome adopts a beads-on-a-string structure, ∼11 nm in diameter, formed by nucleosomes and their linking DNA. This is the building block of the chromatin fiber (2–7). Above the 11-nm fiber, the structure is irregular and dynamically samples a variety of morphologies. Experiments *in vitro*, using DNA templates with uniform arrays of repeating sequences, have shown that chromatin condenses under specific salt conditions to a more compact structure of 30 nm (4,8,9). However, the regularity and existence of this 30-nm fiber *in vivo* continue to be debated (10–13). At length scales on the order of the nuclear domain (micron scale > 100 Mb or mega base pairs), the genome is divided into chromosomes, each of which occupies statistically defined territories. Previous work has shown that polymer models, coupled with confinement in the nucleus and centromere/telomere tethering, capture the essential features of experimental chromosome territories (14–16). These territories are defined statistically, indicative of dynamics of the chromatin chain, implying that the chromosomes are not spatially confined to a given region, rather there is a high probability that they will be found in a specific region (territory) in the nucleus (14–17). At intermediate and large length scales (∼Mb), it is known that the genome is not randomly organized in the nucleus and this spatial organization plays a key role in the execution of a va-

*To whom correspondence should be addressed. Tel: +1 919 962 1182; Fax: +1 919 962 1625; Email: Kerry_Bloom@unc.edu

riety of nuclear functions, e.g. coordinately regulated genes and DNA repair factories (18–20). A key question is to understand the organizational principles that guide the hierarchical organization at this level of compaction. Loops along the polymer chain are one such guiding principle. It has been shown that chromatin loops influence the size and dynamic features of chromosome territories (21–28). Similarly, sub-nuclear compartments and sub-chromosomal interacting domains, such as the nucleolus, gene bodies and topologically associating domains (TADs), play important roles in the organization and dynamic interactions of the genome (29–33); however much remains unknown at this level.

Here, we explore the formation of subdomains in individual live cells during interphase that arise solely from entropy-driven polymeric properties of the nuclear-confined chromatin fiber. We show that entropic fluctuations and excluded volume interactions of confined, tethered polymer chains are sufficient to represent a genome organization that is dynamic, with genes and chromosomal interacting domains varying considerably in time and space and from cell to cell as observed experimentally (34–37). Addition of loops to the model provides a mechanism to tune contact frequencies, also observed experimentally (24). Finally, sub-nuclear compartments offer a mechanism to control interactions at a local level.

Our modeling is based on experimental data from individual, live yeast cells. By quantifying cellular phenomena at this level, we gain a unique perspective on different biological processes that is distinct from the concepts gained by averaging data from populations of cells. Our studies complement those obtained through high-throughput data by extrapolating single cell observations to population averages. The use of dynamic imaging of sub-diffraction chromosomal loci in live cells together with mathematical modeling offers a powerful approach to dissect chromosome interactions in living cells. This approach yields insight into the mechanisms that govern the establishment and maintenance of diverse functional chromatin states in a dynamic cell.

MATERIALS AND METHODS

Modeling approach

Recent results on the diffusive behavior of proteins and DNA *in vivo* suggests that chromatin motion obeys the dynamics of a polymer network (14,38–42). It has also been shown that purely random chain behavior of isolated chromosomes cannot explain many of the specific patterns observed in experiments (14,17,43,44). The question remains whether these patterns arise from generic polymer physics, specific processes such as proteins binding to different sites of the chromatin or higher order organizational principles. Computational simulations show that many of the organizational features observed experimentally emerge from the coupling of the polymer nature of chromatin and simplified geometric constraints (14,15,17,35,36,45–48). These studies investigate different numbers and sizes of chromosomes, confinement to the nuclear space, centromere/telomere tethering and excluded volume effects. We extend these studies to include the formation of loops within chromatin

fibers and the inclusion of sub-nuclear compartments, and explore their impact on global organization as well as local interactions of the genome.

The dynamics of chromatin loci are consistent with those of highly flexible polymers (14,16,17,49–51); for a review of polymer models of interphase chromosomes we refer the reader to (16,42). Accordingly, modeling the four-dimensional behavior of a complex system such as multiple chromatin fibers in the yeast nucleus requires the exploration of a large conformational space. The goal herein is to study the consequences of entropic fluctuations and polymer conformational constraints (confinement, tethering, looping) on the formation of zones of local intrachromosomal interactions. To gain insights into the statistical features of this complex system, we use a simplified, low dimensional, model that captures the essential physics and geometry: a two-dimensional (2D), round nuclear domain and four entropic chains representing four chromosome arms. Results from this simple model are consistent with a three-dimensional (3D) model of the yeast genome (32 chains), as discussed in the supplemental material, thereby providing a simplified context to convey the spatial and dynamic features of chromatin organization.

The dynamics of the chains are modeled using a bead-spring polymer model where the chromosomes are represented by interacting beads connected via springs described by a worm-like chain (WLC) force law (52,53). Each chain is tethered at both ends as shown in Figure 1, representing the tethering of the telomeres to the nuclear membrane and the centromeres to the spindle pole body. This tethering resembles the Rabl configuration observed experimentally (34,47,54–56). In addition to tethering, chains are confined within the nuclear (circular in 2D, spherical in 3D) domain; both constraints reflect *in vivo* observations of yeast chromosomes (14,56). Within this description a segment in a chain represents a 'blob' (57) of chromatin, rather than linear segments. Each blob consists of $N_{k,s}$ Kuhn lengths of length $2L_p$, where L_p is the persistence length of the chromatin fiber. Although a disparate set of values has been reported in the literature for the persistence length of chromatin *in vivo*, ranging from 30 to 220 nm (15,50,58–61); here we consider a persistence length of $L_p = 50$ nm, which corresponds to the persistence length of naked DNA and lies within the reported range for yeast chromosomes. From this perspective it is assumed that the dynamics of the $N_{k,s}$ segments inside each blob follow those of a random walk, forming what is called a Brownian bridge. In this sense, the size of the blobs represents the spatial extent over which the motion of the chromatin fiber is uncorrelated. A detailed description of the model and parameter selection is discussed in the next section.

Model formulation

In the model, the evolution of bead positions is governed by a force balance. In the nucleus, forces controlling molecular interactions include van der Waals (attractive or repulsive), electrostatic (attractive or repulsive), steric (repulsive), hydrodynamic and forces due to thermal fluctuations. In our coarse-grained representation, all attractive forces are captured through a spring-like force and all repulsive effects
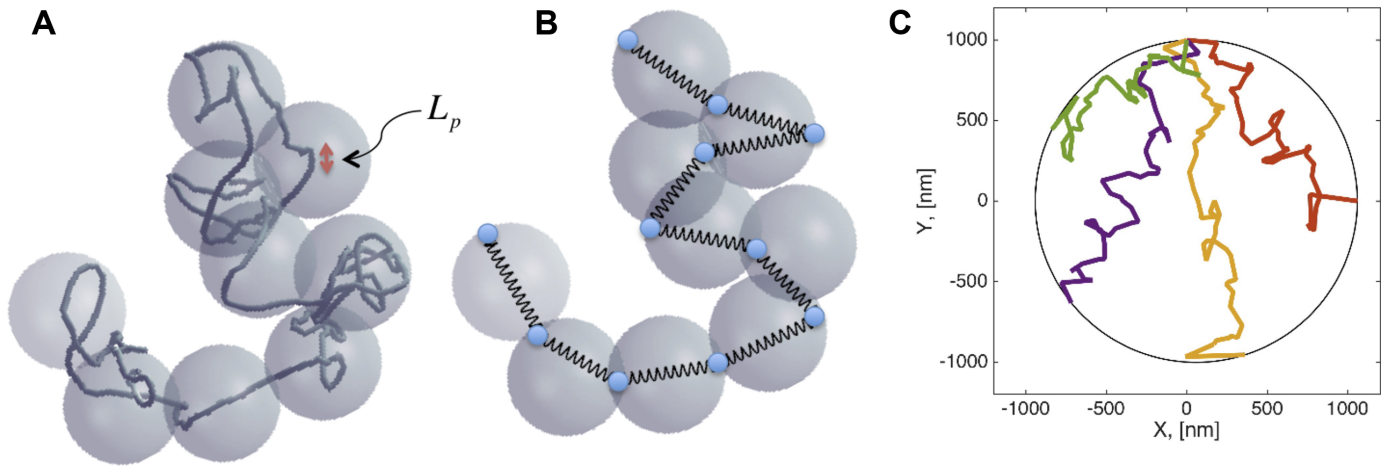
Figure 1. Bead spring representation of chromosome arms. (**A-B**) Each segment, composed by a spring connecting two beads, capture the dynamics of a 'blob'. (**C**) The computational domain consists of four chains, tethered at both ends to a circular domain of radius 1 μm.

by an excluded volume potential. Since the chromatin network is embedded in a highly viscous environment, hydrodynamic interactions (HIs) are also considered. Here, we incorporate viscous drag on the beads and the so-called free draining approximation, as discussed below.

With these simplifications, our formulation is reduced to the balance of five forces acting on each bead,

$$F_i^D + F_i^S + F_i^{EV} + F_i^W + F_i^B = 0. \quad (1)$$

Drag force. The drag force is assumed to follow a linear relation,

$$F_i^D = -\zeta \frac{dX_i}{dt}, \quad (2)$$

where X_i is the vector position of bead i, and ζ is the effective drag coefficient. To determine the drag coefficient we consider the relaxation of a single chain following experiments by Fisher *et al.* (62). In that study the authors found that it takes ∼40 times longer for the chromatin to relax *in vivo*, compared to naked DNA *in vitro*. From this, and based on data from Jendrejack *et al.* (63), we obtain an effective drag coefficient of $\zeta = 2.5 \times 10^{-3}$ pN s/nm.

For simplicity, we omit other types of HIs. Inclusion of HIs in bead-spring models has been shown to be negligible in weak flows (64,65), whereas the flows inside the nucleus are extremely weak. For this reason, and for computational cost considerations, we impose the so-called free draining approximation.

Spring force. This force captures intramolecular interactions via an attractive potential. We use the WLC force proposed by Marko and Siggia (52,53), shown to describe well the dynamics of naked DNA (52,53,63) and chromatin *in vivo* (62),

$$F_i^S = F_{i,j-1} + F_{i,j+1},$$
$$F_{i,j} = \frac{k_B T}{4 L_p} \left[\left(1 - \frac{R_{ij}}{R_0}\right)^{-2} - 1 + 4\frac{R_{ij}}{R_0} \right] \frac{R_{ij}}{R_{ij}}, \quad (3)$$

where,

$$R_{ij} = X_i - X_j, \quad R_{ij} = \sqrt{R_{ij} \cdot R_{ij}}, \quad R_0 = N_{k,s}(2L_p).$$

Excluded volume force. This force imposes an energy penalty on the overlapping of two blobs. In static polymer theory the excluded volume potential is assumed to be a δ-function of the form (66),

$$E(r_j - r_i) = \nu k_B T \delta(r_j - r_i),$$

so that overlapping between two beads has an energy penalty of $\nu k_B T$, where ν is the excluded volume parameter, k_B is the Boltzmann constant and T is the absolute temperature. For our excluded volume potential we use the form proposed by Jendrejack *et al.* (63), where this function is approximated by a narrow Gaussian function:

$$U_i^{EV} = \frac{\nu k_B T}{2} \left(\frac{3}{2\pi S_k^2}\right)^{3/2} \sum_{\substack{i,j=1 \\ i \neq j}}^{N} \exp\left[-\frac{3R_{ij}^2}{2S_k^2}\right], \quad (4)$$

$$F_i^{EV} = -\nabla U_i^{EV},$$

where $S_k^2 = N_{k,s}(2L_p)^2/6$.

Interaction with the cell wall (F_i^w). To account for confinement due to the nuclear envelope, whenever a bead moves outside the domain during a time step, it is moved to the nearest point on the domain boundary as follows,

$$X_i^{\text{new}} = X_i^{\text{out}} + \Delta X_i^{\text{HM}},$$
$$\Delta X_i^{\text{HM}} = \Delta p_i H(\Delta p_i), \quad (5)$$

where ΔX_i^{HM} is the displacement vector due to the Heyes-Melrose algorithm (67), Δp_i is the vector from the position of the bead outside the domain boundary (X_i^{out}) to the nearest boundary point and $H(\cdot)$ is the Heaviside step function.

Brownian force. This force captures random motion due to thermal fluctuations,

$$F_i^B = \sqrt{2\zeta k_B T} dW_i, \quad (6)$$

where dW_i is a standard normal distribution.

Other model parameters

Validation with experimental data. To validate the model parameters we developed a 3D model, consisting of 32 chains corresponding to the arms of the 16 yeast chromosomes. Model settings were selected by matching 3D simulations to experimental data, as discussed in the Supplementary Material. While the 2D model is not appropriate for direct comparison to experimental data, qualitative agreement between the 2D and 3D models, as shown in Figures 2 and 3 and Supplementary Figure S7, demonstrates that even a simplified polymer model can emulate the domains of high chromosomal interaction seen in experimental data. Given the ability of the 2D model to display these results with experimentally derived parameters, the 2D model provides a simplified framework to explore the effects of a large range of parameters on the formation and maintenance of domains of high chromosomal interaction.

Number of beads. The number of beads is related to the level of discretization used to describe a chromosome arm. If we consider the number of kilo base pairs (kb) represented by each spring, $N_{kb} = 5$ and the number of Kuhn lengths per spring, $N_{k,s} = 17$, the number of beads representing a chromosome arm is determined by its length in kb. In our 2D model, we consider chains with 52 beads or equivalently 255 kb. For the 3D model, as explained in the supplemental material, the given length of each chromosome arm determines the number of beads for the different chains, see Supplementary Table S1.

Loops. Chromatin loops impose constraints on chromosome conformation; however, the detailed mechanisms and driving forces of looping are not clear (26,28,68,69). In this work we assume that protein complexes at the base of loops create a spring-like force, dictated by the binding constants within the complex and the DNA. To form loops, we employ a linear spring force and assume that the spring constant has the same order of magnitude as the springs used to form the chains. Lacking experimental information regarding the distribution of co-localized chromatin loci, our first approximation is to distribute them in a uniform manner along the chain. As pointed out by Fudenberg and Mirny (42) this approach falls short of quantitatively capturing experimental observations; however here we show that they suffice, as a first order approximation, to understand the qualitative role of loops in the organization of chromosomes. Furthermore, in spite of this uniform localization, the distribution of loops within the chain is neither fixed nor uniform in time. At a given time, some of the 'looping beads' can be near each other (closed loops) while others can be farther from each other (open loops); this is a consequence of the coupling between the spring forces at the base of the loops and the global dynamics within the domain. An example of this dynamic behavior is shown in Supplementary Figure S11.

Tethering. The first and last beads of each chain correspond to the centromere and telomere sites of a chromosome arm. The position of these beads remain fixed to the boundary throughout the simulations to mimic the attach-

ment of the centromeres to the spindle pole body and telomeres to the nuclear membrane in budding yeast.

RESULTS AND DISCUSSION

Entropic forces acting on chromosome arms generate domains of high intra-chromosomal interactions

In our coarse-grained representation of chromosome arms, the movement of individual beads captures the dynamics of groups of genes. In this sense, analysis of the distance between beads provides the means to make quantitative conclusions about the contact dynamics between genes. We bin the range of interactions represented by averaged separation between beads as shown at the top of Figure 3. We start with the simplest approximation of 208 beads inside a circular domain (representing the nuclear envelope) moving via thermal fluctuations. The beads are independent of each other, meaning the only forces acting on the beads are the confinement force, viscous drag and Brownian forces; these last two are coupled according to the fluctuation-dissipation principle. Figure 3A shows the separation of the beads averaged over 1 h. As expected, there are no preferential interactions between any groups of beads. A quantitative description is given in Figure 3D, which shows the corresponding percentage for the five ranges of separation. In the absence of linkage between beads, the majority of beads remain, on average, separated by distances greater than 750 nm (green and white regions).

To simulate chromosome arms, non-linear springs are introduced between beads (4 chains of 52 beads each) and each chain is attached at both ends (centromere and telomere) to the nuclear envelope as shown in Figure 1C. Figure 3B shows the resulting contact map obtained by averaging bead-to-bead distances. The attractive potential, represented by the spring law, captures intra-chain interactions; for instance an increase in histone occupancy is reproduced by stiffer springs (12). Introduction of chain configurations into the model allows differentiation between intra-chain and inter-chain interactions in the contact maps (Figure 3D). The addition of springs effectively decreases the number of possible configurations for the 208 beads, which in turn decreases the entropy of the system. In other words, a decrease in the system's entropy results in an increase in local interactions. This is represented in Figure 3D by an increase in the percentage of blue (500–750 nm separation) and black (250–500 nm separation) regions. We note that 500 nm is the radius of gyration (R_g) of a 20 kb random coil of DNA: $R_g = \sqrt{N(2L_p)^2/6}$, validating the estimate of bead separation and the black regions as domains with high bead-bead interactions mimicking TADs.

Finally, excluded volume interactions are incorporated into the model and the resulting contact map is shown in Figure 3C. Excluded volume is a mathematical construct that captures the physical basis for molecular exclusion, which is about $8\times$ the intrinsic volume of the polymer chain (70). Addition of this repulsive potential further reduces the degrees of freedom in chain configurations and accordingly the entropy of the system. This additional reduction in entropy results in a decrease of inter-chain interactions, as shown by the increase in the percentage of white regions
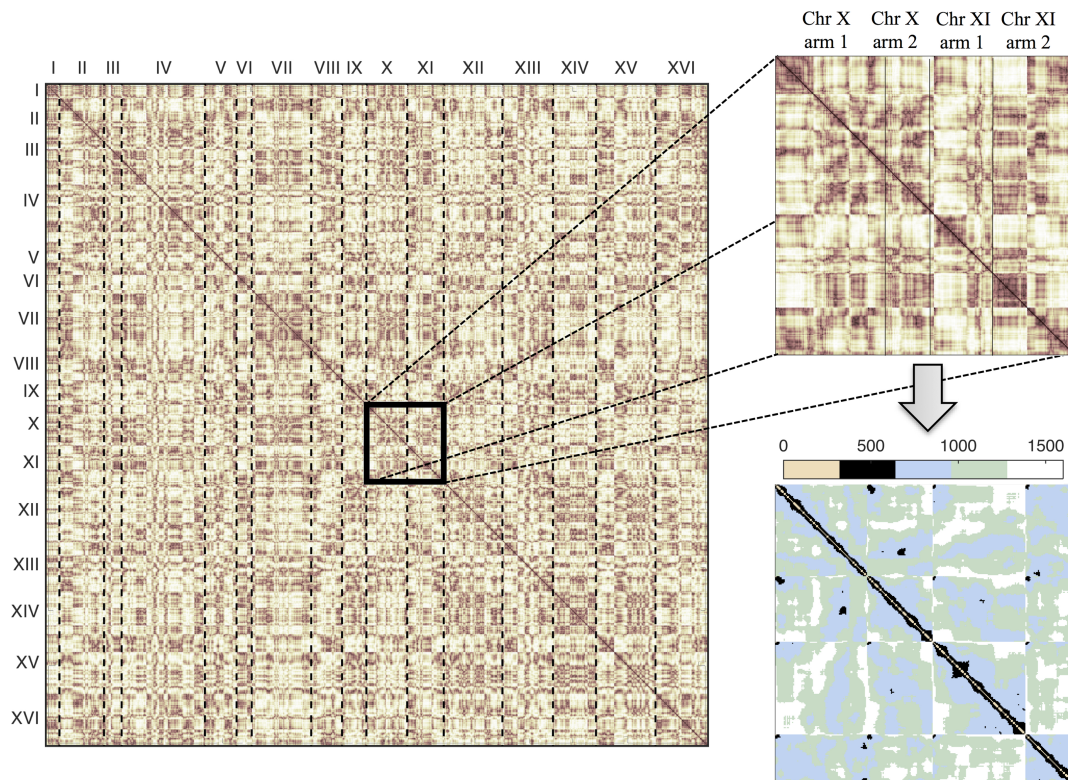
Figure 2. Average separation between beads in the 3D model (2443 beads). The behavior of four selected chains agrees *qualitatively* with the behavior obtained for the 2D, four-chains model (see Figure 3 and Supplementary Figure S7).

(>1000 nm separation) within the inter-chain plot of Figure 3D.

Numerical simulations of polymer models have shown that, in addition to tethering, the spatial organization of chromosomes is regulated by excluded volume effects. The latter becomes crucial when confinement is introduced, as chromosomes 'compete' for the limited nuclear space (14–17). In this context, the changes in inter- and intra-chromosomal interactions shown in Figure 3 are not surprising. The main conclusion from Figure 3 is the formation of high-frequency intra-chain interactions, as the black regions within the contact maps imply that those beads remain on average separated by <500 nm over the course of 1 h. By modeling chromosome arms as polymer chains (bead-spring model) interacting via entropic potentials, such as the spring and excluded volume forces, we have shown that domains of high interaction arise naturally in the system without the need for other mechanical or chemical potentials. However, these regions are not static and vary from cell to cell (Supplementary Movie 1).

Finally, we note that previous work argues that loops are responsible for both the formation of chromosome territories and TADs (26,51). Here, we argue that loops, or any other type of contact dynamics, are not necessary to create these domains, as they arise from first principles. Below we show that the role of loops is to modulate these domains by reducing the conformational degrees of freedom of the chains.

Changes in chain configuration through the addition of loops result in compartmentalization of chain interactions

A distinguishing feature of eukaryotic chromosomes is an underlying scaffold from which a series of chromatin loops emanate (21,23,25). Loops represent mechanisms to confine topologies to sub-regions of the chromosome providing structural differentiation for processes such as transcription, replication and repair. To examine the consequences of loops in the entropic model, we implemented linear springs connecting specific pairs of beads along each chain. The resulting contact maps are shown for two different loop configurations in Figure 4. To assess the changes imposed in the system, simulations were run using the same thermal noise with and without loops. In this manner, subtraction of bead distances, as shown in Supplementary Figure S1, exposes changes arising solely from loop dynamics. These changes are divided in three main categories: distances between beads in the backbone, distances between beads in the outer loops and distances between beads in the backbone and beads in the outer loops; each is shown in the bar plots of Figure 4. We further consider intra- and inter-chain distances dividing each bar plot into these two categories.

Figure 4 shows that the majority of the interactions remain unchanged after the addition of loops (gray bars). The next largest change comes from beads in the backbone of the same chain (blue bars, intra-chain), since loops in the chain bring the backbone beads closer. In addition, distances between beads in different chains increase (red bars, inter-chain). The fact that this change is the same in both
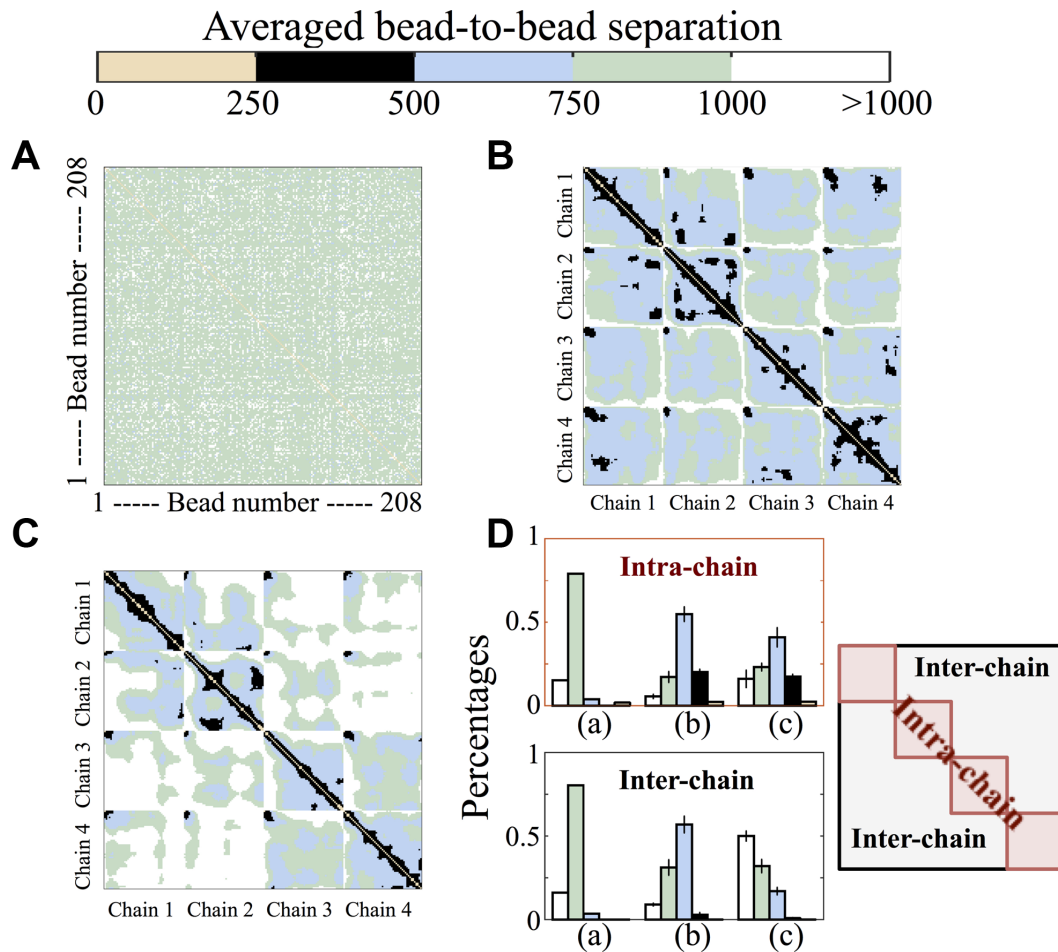
Figure 3. Heat maps of distances between beads averaged over 1 h and divided into five regions according to the mean bead-to-bead separation. (**A**) Beads confined to a circle of radius 1 micron and moving through Brownian motion. (**B**) An attractive potential (worm-like spring) is added to the same noise history as in (A). The addition of this potential also allow the division of the 208 beads into four chains as shown in Figure 1C. (**C**) Inter-molecular interactions are added to the same simulation through an excluded volume potential. In addition to steric effects, this force also captures any type of repulsion between different beads. (**D**) Percentage of the five bead-to-bead separation areas for figures (A), (B) and (C), separated according to intra- and inter-chain regions as shown in the inset.

outer-loop and backbone beads suggests an enhancement in chromosome territories. To further illustrate this, we plot the positions of beads with and without loops and show that indeed chromosome territories are more defined with loops (Supplementary Figure S2). Thus chromosome loops increase a chromosome arm's individuality, in agreement with previous studies (26,51).

Loops arise from several different sources *in vivo*. Cohesin together with CTCF (CCCTC-binding factor) are found in many organisms to tether distant sites and promote expression of the intervening genes (33,71–73). Condensin along with tDNA (DNA encoding transfer RNA (tRNA) genes) and rDNA (ribosomal DNA) transcription factors function to bridge distant sequences in the nucleolus of most organisms (74,75), as well as pericentric chromatin in yeast (40,76). We refer to these complexes in general as *topology adjusters* (77). The finding herein indicates that rather than *de novo* creation of subdomain with high interactions, these complexes enhance and extend the duration of domains that stochastically arise from the entropic interactions of the chromosome arms in a confined domain.

It will be important in future extensions of the model to explicitly include the stochastic dynamics of these complexes and their interactions with chromosome arms as their biophysical properties become better understood. However, it is clear that such topology adjusters such as cohesin and condensin bias the longevity of naturally 'transient' loops, thus influencing the overall genome architecture (Supplementary Figures S3 and 4).

To test whether loops alone can modify the territory of a given chromosome, we introduce loops in only one of the four chains. The data is shown in Figure 5. Addition of loops in only one chain results in a decrease of the intra-chain distances, but only for the chain with loops. This implies that the extent of the territory for that given chain is reduced, while other territories remain unchanged. Furthermore, increase in inter-chain distances also implies that loops serve as a mechanism to isolate individual chains to increase interactions within the chain and to decrease interaction with other chains. These changes in distances are quantified in Supplementary Figure S3.
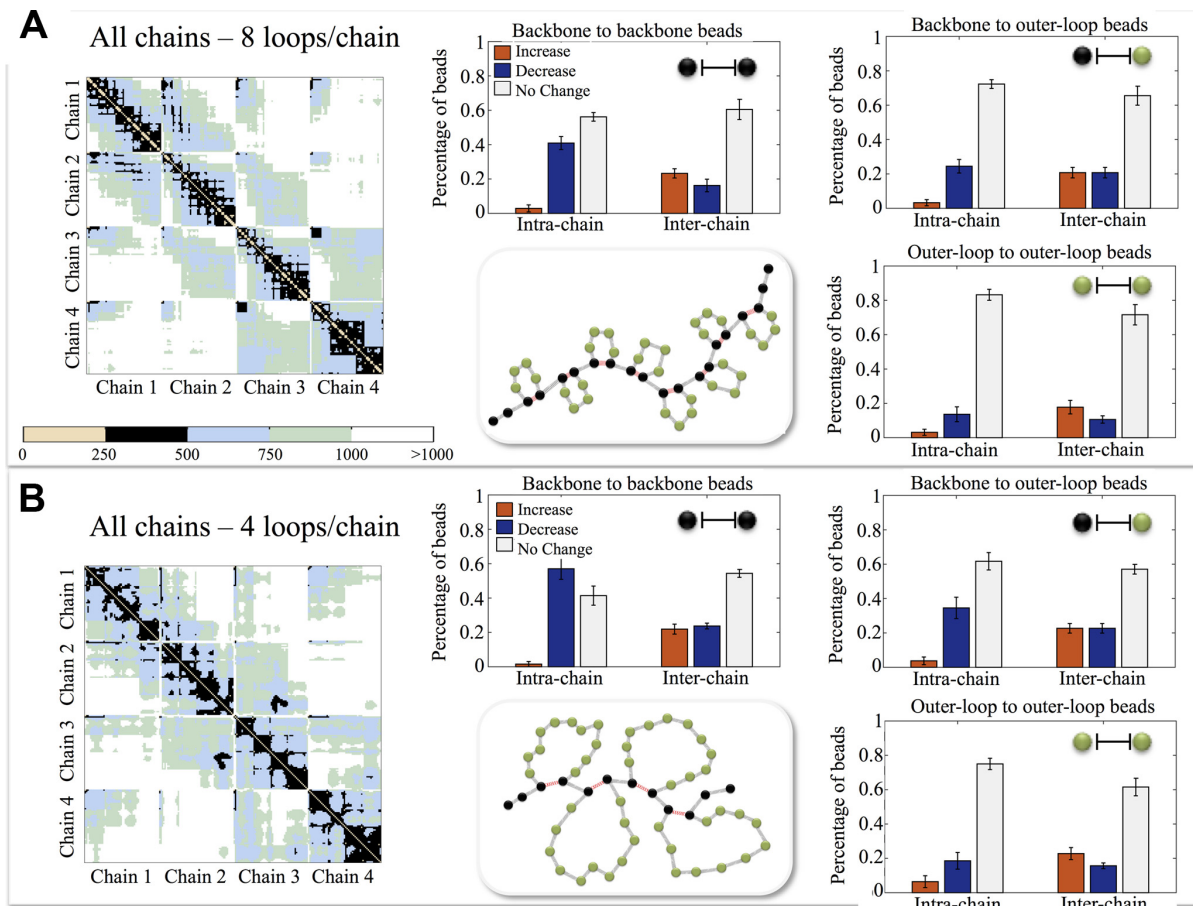
Figure 4. Contact maps for different conformations that include loops and changes in the average distance between beads. Bead interactions are divided into backbone-to-backbone (dark beads), outer loop-to-outer loop (light beads) and backbone-to-outer loop. Intra-chain interactions are given by the 'same chain' bars, while inter-chain interactions correspond to 'different chain' bars. Shades of the bars correspond to increase, decrease and no change in the distance between two beads due to the presence of loops. These bars correspond to the regions discussed in Supplementary Figure S8. (**A**) Chain conformation consists of eight loops per chain, each loop comprising six beads. (**B**) Chains are organized into four loops per chain, each loop with 13 beads. Calculation of the changes in the average distance is described in Supplementary Figure S8.

Nuclear bodies are secondary levels of regulation of subdomains of high intra-chromosomal interactions

In addition to loops, the cell can employ other secondary mechanisms to bias genome architecture toward a given state. Figure 6 explores two such mechanisms: the first one introduces a nuclear body by defining a circular sub-domain within the cell that beads cannot penetrate (Figure 6B); the second one is similar to the previous nuclear body, but, in addition, a set of beads belonging to one chain is confined to the sub-domain (Figure 6C). Comparison of the resulting contact maps clearly shows that these nuclear bodies only affect genome interactions at a local level, independent of whether or not the chains have a linear or a loop configuration. As discussed in the previous section, the addition of loops results in enhanced isolation for the regions of high bead-interactions and smaller modifications to the interactions in the rest of the nucleus.

CONCLUSION

Critical chromosomal functions have been linked to the spatial conformation of chromosomes. While sequencing-based techniques such as Hi-C provide an overall impression of genome organization, as pointed out in (42), a large number of contacts observed in Hi-C data does not imply a specific physical or functional interaction between the contacting loci. Rather, mechanistic models of chromatin are necessary to deduce the major physical influences on genome organization. Using mathematical models, we investigated the role that entropic forces, confinement and chromatin looping play in the formation of domains of higher order chromosomal interactions. A persistent view is that this spatial organization is primarily established by enzymatic, protein-guided cellular processes. Here we showed that entropy and the fundamental polymeric nature of chromatin dictate the structure and dynamics of the genome. The role of proteins is to guide, stabilize and sustain cycle-specific genome states.

An important feature of protein-guided chromatin organization is chromatin looping. In addition to their role in the organization of interphase chromatin, loop formation has been shown to play an important role in models of meiotic and mitotic chromosomes (78,79). In contrast to the work of Bohn and Heermann (26), the loops in our model
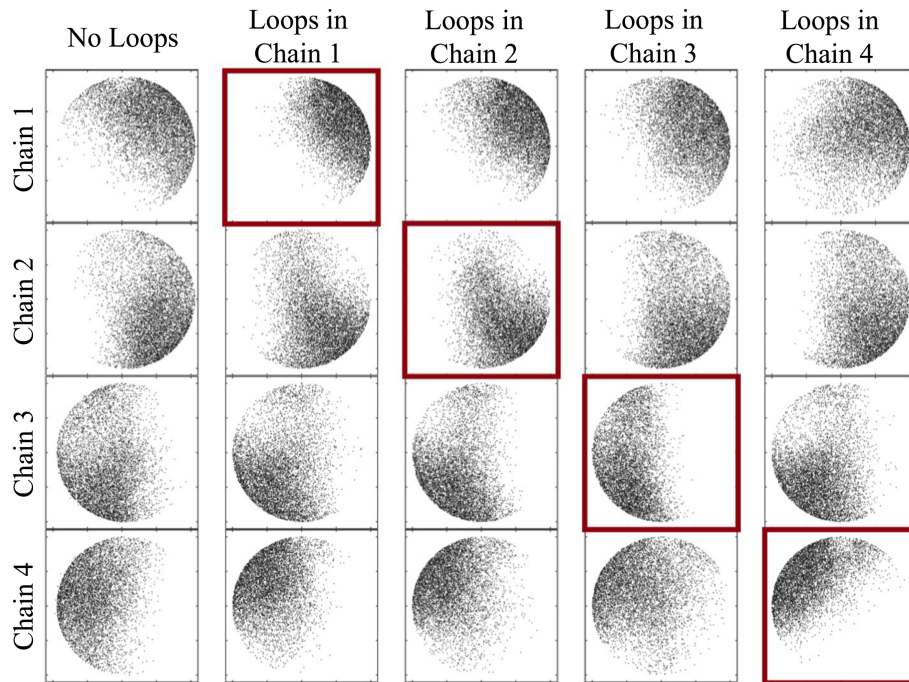
Figure 5. Chain's territories as a function of chain configuration. Rows correspond to territories of the same chain, columns correspond to different configurations, from left to right: no loops, loops only in chain 1, loops only in chain 2, loops only in chain 3 and loops only in chain 4. A quantitative analysis of the change in bead-to-bead distances is given in Supplementary Figure S10.
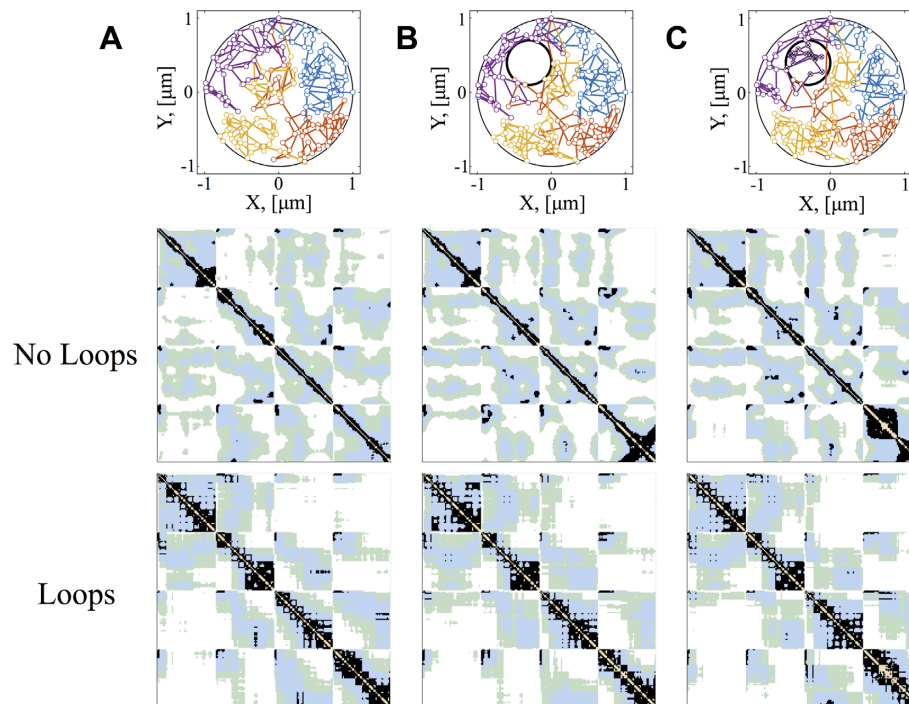
Figure 6. Secondary levels of regulation of intra-chain interactions. (**A**) Simulation without of nuclear bodies and resulting contact maps for chains without and with loops. (**B**) Simulations where beads are excluded from a circular region of radius 300 nm placed inside the nucleus (radius 1000 nm). (**C**) Simulations where most beads are excluded from a circular region while beads 15–30 from chain 4 (purple) are confined to the sub-domain.

are mediated by long-range interactions (linear springs). In (26) the authors showed that 'the formation of loops can be accomplished solely on the basis of diffusional motion.' A next step in the refinement of genome models is to introduce the dynamics for the formation and modulation of loops and to investigate their role in the spatial organization and interaction of the yeast genome. Furthermore, as the biological understanding of specific DNA–protein interactions increase, future models of dynamic genome organization will need to incorporate these interactions to better understand how proteins adjust an entropically-organized genome. In this way, mathematical models of genome organization, together with live cell experiments, will identify genomic signatures that define cell states and protein functions.

SUPPLEMENTARY DATA

Supplementary Data are available at NAR Online.

REFERENCES

1. Ea,V., Baudement,M.-O., Lesne,A. and Forné,T. (2015) Contribution of topological domains and loop formation to 3D chromatin organization. *Genes*, **6**, 734–750.
2. Chakravarthy,S., Park,Y.-J., Chodaparambil,J., Edayathumangalam,R.S. and Luger,K. (2005) Structure and dynamic properties of nucleosome core particles. *FEBS Lett.*, **579**, 895–898.
3. Chodaparambil,J.V., Edayathumangalam,R.S., Bao,Y., Park,Y.-J. and Luger,K. (2006) Nucleosome structure and function. In: *The Histone Code and Beyond*. Springer, Berlin Heidelberg, pp. 29–46.
4. McGhee,J.D., Rau,D.C., Charney,E. and Felsenfeld,G. (1980) Orientation of the nucleosome within the higher order structure of chromatin. *Cell*, **22**, 87–96.
5. McGinty,R.K. and Tan,S. (2014) Nucleosome structure and function. *Chem. Rev.*, **115**, 2255–2273.
6. Schiessel,H. (2003) The physics of chromatin. *J. Phys. Condens. Matter*, **15**, R699–R774.
7. Wolffe,A. (1998) *Chromatin: structure and function*. Academic press, London.
8. Allahverdi,A., Chen,Q., Korolev,N. and Nordenskiöld,L. (2015) Chromatin compaction under mixed salt conditions: opposite effects of sodium and potassium ions on nucleosome array folding. *Sci. Rep.*, **5**, 1–7.
9. Van Holde,K. and Zlatanova,J. (1996) What determines the folding of the chromatin fiber? *Proc. Natl. Acad. Sci.*, **93**, 10548–10555.
10. van Holde,K. and Zlatanova,J. (1995) Chromatin higher order structure: chasing a mirage? *J. Biol. Chem.*, **270**, 8373–8376.
11. Woodcock,C.L., Frado,L.-L. and Rattner,J.B. (1984) The higher-order structure of chromatin: evidence for a helical ribbon arrangement. *J. Cell Biol.*, **99**, 42–52.
12. Fussner,E., Ching,R.W. and Bazett-Jones,D.P. (2011) Living without 30nm chromatin fibers. *Trends Biochem. Sci.*, **36**, 1–6.
13. Eltsov,M., MacLellan,K.M., Maeshima,K., Frangakis,A.S. and Dubochet,J. (2008) Analysis of cryo-electron microscopy images does not support the existence of 30-nm chromatin fibers in mitotic chromosomes in situ. *Proc. Natl. Acad. Sci.*, **105**, 19732–19737.
14. Verdaasdonk,J.S., Vasquez,P.A., Barry,R.M., Barry,T., Goodwin,S., Forest,M.G. and Bloom,K. (2013) Centromere tethering confines chromosome domains. *Mol. Cell*, **52**, 819–831.
15. Tjong,H., Gong,K., Chen,L. and Alber,F. (2012) Physical tethering and volume exclusion determine higher-order genome organization in budding yeast. *Genome Res.*, **22**, 1295–1305.
16. Wang,R., Mozziconacci,J., Bancaud,A. and Gadal,O. (2015) Principles of chromatin organization in yeast: relevance of polymer models to describe nuclear organization and dynamics. *Curr. Opin. Cell Biol.*, **34**, 54–60.
17. Vasquez,P.A. and Bloom,K. (2014) Polymer models of interphase chromosomes. *Nucleus*, **5**, 376–390
18. Misteli,T. and Soutoglou,E. (2009) The emerging role of nuclear architecture in DNA repair and genome maintenance. *Nat. Rev. Mol. Cell Biol.*, **10**, 243–254.
19. Taddei,A., Schober,H. and Gasser,S.M. (2010) The budding yeast nucleus. *Cold Spring Harb. Perspect. Biol.*, **2**, a000612.
20. Takizawa,T., Meaburn,K.J. and Misteli,T. (2008) The meaning of gene positioning. *Cell*, **135**, 9–13.
21. Alipour,E. and Marko,J.F. (2012) Self-organization of domain structures by DNA-loop-extruding enzymes. *Nucleic Acids Res.*, **40**, 11202–11212.
22. Giles,K.E., Gowher,H., Ghirlando,R., Jin,C. and Felsenfeld,G. (2010) Chromatin boundaries, insulators, and long-range interactions in the nucleus. In: *Cold Spring Harbor symposia on quantitative biology*. Cold Spring Harbor Laboratory Press, NY, Vol. 75, pp. 7985.
23. Kagey,M.H., Newman,J.J., Bilodeau,S., Zhan,Y., Orlando,D.A., van Berkum,N.L., Ebmeier,C.C., Goossens,J., Rahl,P.B., Levine,S.S. *et al.* (2010) Mediator and cohesin connect gene expression and chromatin architecture. *Nature*, **467**, 430–435.
24. Rao,S.S., Huntley,M.H., Durand,N.C., Stamenova,E.K., Bochkov,I.D., Robinson,J.T., Sanborn,A.L., Machol,I., Omer,A.D. and Lander,E.S. (2014) A 3D map of the human genome at kilobase resolution reveals principles of chromatin looping. *Cell*, **159**, 1665–1680.
25. Schleif,R. (1992) DNA looping. *Annu. Rev. Biochem.*, **61**, 199–223.
26. Bohn,M. and Heermann,D.W. (2010) Diffusion-driven looping provides a consistent framework for chromatin organization. *PLoS One*, **5**, e12218.
27. Tark-Dame,M., Jerabek,H., Manders,E.M., Heermann,D.W. and van Driel,R. (2014) Depletion of the chromatin looping proteins CTCF and cohesin causes chromatin compaction: insight into chromatin folding by polymer modelling. *PLoS Comput. Biol.*, **10**, e1003877.
28. Doyle,B., Fudenberg,G., Imakaev,M. and Mirny,L.A. (2014) Chromatin loops as allosteric modulators of enhancer-promoter interactions. *PLoS Comput. Biol.*, **10**, e1003867.
29. Dekker,J., Marti-Renom,M.A. and Mirny,L.A. (2013) Exploring the three-dimensional organization of genomes: interpreting chromatin interaction data. *Nat. Rev. Genet.*, **14**, 390–403.
30. Dixon,J.R., Selvaraj,S., Yue,F., Kim,A., Li,Y., Shen,Y., Hu,M., Liu,J.S. and Ren,B. (2012) Topological domains in mammalian genomes identified by analysis of chromatin interactions. *Nature*, **485**, 376–380.
31. Lupiáñez,D.G., Kraft,K., Heinrich,V., Krawitz,P., Brancati,F., Klopocki,E., Horn,D., Kayserili,H., Opitz,J.M. and Laxova,R. (2015) Disruptions of topological chromatin domains cause pathogenic rewiring of gene-enhancer interactions. *Cell*, **161**, 1012–1025.
32. Nora,E.P., Dekker,J. and Heard,E. (2013) Segmental folding of chromosomes: a basis for structural and regulatory chromosomal neighborhoods? *Bioessays*, **35**, 818–828.
33. Ong,C.-T. and Corces,V.G. (2014) CTCF: an architectural protein bridging genome topology and function. *Nat. Rev. Genet.*, **15**, 234–246.
34. Berger,A.B., Cabal,G.G., Fabre,E., Duong,T., Buc,H., Nehrbass,U., Olivo-Marin,J.-C., Gadal,O. and Zimmer,C. (2008) High-resolution statistical mapping reveals gene territories in live yeast. *Nat. Methods*, **5**, 1031–1037.

35. Heun,P., Laroche,T., Shimada,K., Furrer,P. and Gasser,S.M. (2001) Chromosome dynamics in the yeast interphase nucleus. *Science*, **294**, 2181–2186.

36. Marshall,W.F., Straight,A., Marko,J.F., Swedlow,J., Dernburg,A., Belmont,A., Murray,A.W., Agard,D.A. and Sedat,J.W. (1997) Interphase chromosomes undergo constrained diffusional motion in living cells. *Curr. Biol.*, **7**, 930–939.

37. Wong,H., Arbona,J.-M. and Zimmer,C. (2013) How to build a yeast nucleus. *Nucleus*, **4**, 361–366.

38. Erdel,F., Baum,M. and Rippe,K. (2015) The viscoelastic properties of chromatin and the nucleoplasm revealed by scale-dependent protein mobility. *J. Phys. Condens. Matter*, **27**, 064115.

39. Lawrimore,J., Vasquez,P.A., Falvo,M.R., Taylor,R.M., Vicci,L., Yeh,E., Forest,M.G. and Bloom,K. (2015) DNA loops generate intracentromere tension in mitosis. *J. Cell Biol.*, **210**, 553–564.

40. Stephens,A.D., Haggerty,R.A., Vasquez,P.A., Vicci,L., Snider,C.E., Shi,F., Quammen,C., Mullins,C., Haase,J., Taylor,R.M. *et al.* (2013) Pericentric chromatin loops function as a nonlinear spring in mitotic force balance. *J. Cell Biol.*, **200**, 757–772.

41. Stephens,A.D., Snider,C.E., Haase,J., Haggerty,R.A., Vasquez,P.A., Forest,M.G. and Bloom,K. (2013) Individual pericentromeres display coordinated motion and stretching in the yeast spindle. *J. Cell Biol.*, **203**, 407–416.

42. Fudenberg,G. and Mirny,L.A. (2012) Higher-order chromatin structure: bridging physics and biology. *Curr. Opin. Genet. Dev.*, **22**, 115–124.

43. Rosa,A., Becker,N.B. and Everaers,R. (2010) Looping probabilities in model interphase chromosomes. *Biophys. J.*, **98**, 2410–2419.

44. Perkins,T.T., Smith,D.E. and Chu,S. (1997) Single polymer dynamics in an elongational flow. *Science*, **276**, 2016–2021.

45. Bystricky,K., Laroche,T., van Houwe,G., Blaszczyk,M. and Gasser,S.M. (2005) Chromosome looping in yeast telomere pairing and coordinated movement reflect anchoring efficiency and territorial organization. *J. Cell Biol.*, **168**, 375–387.

46. Rosa,A. and Everaers,R. (2008) Structure and dynamics of interphase chromosomes. *PLoS Comput. Biol.*, **4**, e1000153.

47. Therizols,P., Duong,T., Dujon,B., Zimmer,C. and Fabre,E. (2010) Chromosome arm length and nuclear constraints determine the dynamic relationship of yeast subtelomeres. *Proc. Natl. Acad. Sci.*, **107**, 2025–2030.

48. Wong,H., Marie-Nelly,H., Herbert,S., Carrivain,P., Blanc,H., Koszul,R., Fabre,E. and Zimmer,C. (2012) A predictive computational model of the dynamic 3D interphase yeast nucleus. *Curr. Biol.*, **22**, 1881–1890.

49. Albert,B., Mathon,J., Shukla,A., Saad,H., Normand,C., Léger-Silvestre,I., Villa,D., Kamgoue,A., Mozziconacci,J. and Wong,H. (2013) Systematic characterization of the conformation and dynamics of budding yeast chromosome XII. *J. Cell Biol.*, **202**, 201–210.

50. Hajjoul,H., Mathon,J., Ranchon,H., Goiffon,I., Mozziconacci,J., Albert,B., Carrivain,P., Victor,J.-M., Gadal,O. and Bystricky,K. (2013) High-throughput chromatin motion tracking in living yeast reveals the flexibility of the fiber throughout the genome. *Genome Res.*, **23**, 1829–1838.

51. Cheng,T.M., Heeger,S., Chaleil,R.A., Matthews,N., Stewart,A., Wright,J., Lim,C., Bates,P.A. and Uhlmann,F. (2015) A simple biophysical model emulates budding yeast chromosome condensation. *Elife*, **4**, e05565.

52. Marko,J.F. and Siggia,E.D. (1994) Bending and twisting elasticity of DNA. *Macromolecules*, **27**, 981–988.

53. Marko,J.F. and Siggia,E.D. (1995) Stretching DNA. *Macromolecules*, **28**, 8759–8770.

54. Dekker,J., Rippe,K., Dekker,M. and Kleckner,N. (2002) Capturing chromosome conformation. *Science*, **295**, 1306–1311.

55. Duan,Z., Andronescu,M., Schutz,K., McIlwain,S., Kim,Y.J., Lee,C., Shendure,J., Fields,S., Blau,C.A. and Noble,W.S. (2010) A three-dimensional model of the yeast genome. *Nature*, **465**, 363–367.

56. Zimmer,C. and Fabre,E. (2011) Principles of chromosomal organization: lessons from yeast. *J. Cell Biol.*, **192**, 723–733.

57. De Gennes,P.-G. (1979) *Scaling concepts in polymer physics*. Cornell university press, NY.

58. Bystricky,K., Heun,P., Gehlen,L., Langowski,J. and Gasser,S.M. (2004) Long-range compaction and flexibility of interphase chromatin in budding yeast analyzed by high-resolution imaging techniques. *Proc. Natl. Acad. Sci. U.S.A.*, **101**, 16495–16500.

59. Cui,Y. and Bustamante,C. (2000) Pulling a single chromatin fiber reveals the forces that maintain its higher-order structure. *Proc. Natl. Acad. Sci. U.S.A.*, **97**, 127–132.

60. Langowski,J. (2006) Polymer chain models of DNA and chromatin. *Euro. Phys. J. E*, **19**, 241–249.

61. Dekker,J. (2008) Mapping in vivo chromatin interactions in yeast suggests an extended chromatin fiber with regional variation in compaction. *J. Biol. Chem.*, **283**, 34532–34540.

62. Fisher,J.K., Ballenger,M., O'Brien,E.T., Haase,J., Superfine,R. and Bloom,K. (2009) DNA relaxation dynamics as a probe for the intracellular environment. *Proc. Natl. Acad. Sci. U.S.A.*, **106**, 9250–9255.

63. Jendrejack,R.M., de Pablo,J.J. and Graham,M.D. (2002) Stochastic simulations of DNA in flow: dynamics and the effects of hydrodynamic interactions. *J. Chem. Phys.*, **116**, 7752–7759.

64. Larson,R.G. (2005) The rheology of dilute solutions of flexible polymers: progress and problems. *J. Rheol.*, **49**, 1–70.

65. Underhill,P.T. and Doyle,P.S. (2007) Accuracy of bead-spring chains in strong flows. *J. Non-Newtonian Fluid Mech.*, **145**, 109–123.

66. Doi,M. and Edwards,S.F. (1986) *The theory of polymer dynamics*. Claredon, Oxford.

67. Heyes,D.M. and Melrose,J.R. (1993) Brownian dynamics simulations of model hard-sphere suspensions. *J. Non-Newtonian Fluid Mech.*, **46**, 1–28.

68. Rippe,K. (2001) Making contacts on a nucleic acid polymer. *Trends Biochem. Sci.*, **26**, 733–740.

69. Sachs,R.K., Van Den Engh,G., Trask,B., Yokota,H. and Hearst,J.E. (1995) A random-walk/giant-loop model for interphase chromosomes. *Proc. Natl. Acad. Sci. U.S.A.*, **92**, 2710–2714.

70. Hancock,R. (2014) The crowded nucleus. In: *New models of the cell nucleus: crowding, entropic forces, phase separation, and fractals*. Academic Press, Cambridge, Vol. **307**, pp. 15–26.

71. Ghirlando,R. and Felsenfeld,G. (2016) CTCF: making the right connections. *Genes Dev.*, **30**, 881–891.

72. Hou,C., Dale,R. and Dean,A. (2010) Cell type specificity of chromatin organization mediated by CTCF and cohesin. *Proc. Natl. Acad. Sci. U.S.A.*, **107**, 3651–3656.

73. Phillips,J.E. and Corces,V.G. (2009) CTCF: master weaver of the genome. *Cell*, **137**, 1194–1211.

74. Chen,M. and Gartenberg,M.R. (2014) Coordination of tRNA transcription with export at nuclear pore complexes in budding yeast. *Genes Dev.*, **28**, 959–970.

75. Haeusler,R.A., Pratt-Hyatt,M., Good,P.D., Gipson,T.A. and Engelke,D.R. (2008) Clustering of yeast tRNA genes is mediated by specific association of condensin with tRNA gene transcription complexes. *Genes Dev.*, **22**, 2204–2214.

76. Snider,C.E., Stephens,A.D., Kirkland,J.G., Hamdani,O., Kamakaka,R.T. and Bloom,K. (2014) Dyskerin, tRNA genes, and condensin tether pericentric chromatin to the spindle axis in mitosis. *J. Cell Biol.*, **207**, 189–199.

77. Bloom,K. and Joglekar,A. (2010) Towards building a chromosome segregation machine. *Nature*, **463**, 446–456.

78. Marko,J.F. and Siggia,E.D. (1997) Polymer models of meiotic and mitotic chromosomes. *Mol. Biol. Cell*, **8**, 2217–2231.

79. Marshall,W.F. and Fung,J.C. (2016) Modeling meiotic chromosome pairing: nuclear envelope attachment, telomere-led active random motion, and anomalous diffusion. *Phys. Biol.*, **13**, 026003.